Anal. Bioanal. Electrochem., Vol. 13, No. 1, 2021, 127-138

Analytical &
Bioanalytical
Electrochemistry

2021 by CEE
www.abechem.com

Full Paper

Preparation of Antimony Oxide in Different Media and Its Effect on the pH Measurement

Shova Neupane,[1],* Dinesh Mishra,[1] Krishna Badan Nakarmi,[1] Dipak Kumar Gupta,[1] Ram Jeewan Yadav,[2] and Amar Prasad Yadav[1],*

[1] *Central Department of Chemistry, Tribhuvan University, Kirtipur, Kathmandu, Nepal*

[2] *Department of Chemistry, Prithivi Narayan Campus, Tribhuvan University, Pokhara, Nepal*

*Corresponding Author, Tel.: +9779851124444

E-mails: shova_n@yahoo.com (Shova Neupane); amar2y@yahoo.com (Amar Prasad Yadav)

Received: 7 November 2020 / Received in revised form: 30 December 2020 / Accepted: 31 July 2021 / Published online: 31 August 2021

Abstract- A thin film of antimony-oxide on an antimony electrode (Sb-Sb-oxide) is a simple, robust, and low-cost electrode for pH measurement. This study reports on the effect of different electrolytic media on forming a thin-film of Sb-oxide by electrochemical methods and its stability for pH measurements. An antimony electrode was obtained by the melting and solidification of antimony powder. Sb-oxide, thus obtained by electrochemical methods, was characterized by X-ray Photoelectron Spectroscopy (XPS). The cyclic voltammetry (CV) study revealed a complex oxide formation mechanism. This mechanism could be interpreted as a stepwise formation of different Sb species, such as Sb_2O_3 and Sb_2O_5, in a low field near an open circuit potential (OCP). XPS results showed that the Sb_2O_3 and Sb_2O_5 ratio was almost similar in acidic medium, whereas Sb_2O_5 was dominant in phosphate solution. All the prepared Sb-Sb-oxide electrodes showed a linear electromotive force (*e.m.f.*) in pH 2-10, giving a slope of 0.049- 0.052 V/pH at room temperature (RT). The electrodes gave an excellent pH response, and hence they can be used in standard laboratory experiments where the accuracy of ±0.02 pH is required. However, Sb-oxide obtained in phosphate buffer solution of pH 7 showed a lower electrode sensitivity and lower stability due to dominant Sb_2O_5 formation.

Keywords- Potentiostatic Polarization; Open-circuit Potential; Cyclic Voltammetry; X-ray Photoelectron Spectroscopy

1. INTRODUCTION

Metal-metal oxide-based electrodes have been prepared and used as a pH sensor for aqueous electrolytes for a long [1,2]. A thin film of insoluble metal oxide is formed as soon as certain noble metals such as bismuth, tin, tungsten, tellurium, and antimony are immersed in an electrolyte at room temperature (RT). These metal oxides form a redox couple, which shows quick, reversible, and reproducible responses towards hydrogen ion concentrations. The potential drift during pH measurement is small and comes into equilibrium without appreciable dissolutions of oxides [3,4]. In the recent past, there has been increasing interest in the metal-metal oxides as pH electrodes due to greater rigidity, low impedance, and high scope for miniaturization [5]. Besides these, metal-metal oxide electrodes are easy to handle, and they can be readily fabricated on single crystals or polycrystalline metals in the laboratory at RT.

A glass electrode is the most commonly used pH sensor because of its comprehensive range of pH, freedom from oxidation-reduction ("redox"), and other interferences [6]. These electrodes have certain materials and design limitations, such as fragility, high impedance, and the need for an internal aqueous phase. This precludes the straight forward miniaturization and microfabrication of glass pH electrodes. At the same time, it is inconvenient to use and difficult to prepare; therefore, the glass electrode is not adopted for general measurement [7,8]. Alternatively, a quinhydrone electrode has also been tried, but contamination of the test solution with quinhydrone itself is a problem. Therefore, the combination of glass electrodes with metal-metal oxide electrodes is used for pH measurements to overcome these drawbacks [9–11]. The metal-metal oxide electrodes are being optimized and prepared using polymers, nanotubes, and several compositions to increase their efficiency [12–15].

Among the different metal-metal oxide electrodes, the antimony-antimony oxide (Sb-Sb-oxide) electrode is one of the most well-behaved electrodes for pH determination [4,10,11,16–18]. The equation may represent the basic reaction of the Sb-Sb-oxide electrode for hydrogen ion concentration:

$$Sb_2O_3 + 6H^+ + 6e^- \rightarrow Sb + 3H_2O$$

The Nernst equation gives the electrode potential as:

$$E_{Sb} = E^o - (^{RT}/_{6F}) \ln {}^1/a^6{}_{H^+}$$
$$= E^o - 0.0591 \text{ pH} \quad (\text{at } 25^oC)$$

Several characterizations and optimizations have been done by many researchers dealing with the different aspects of the Sb-Sb-oxide electrode for pH measurements [6–8]. The growth of antimony oxide and the evolution of its morphology were studied. The stability of the prepared electrode in buffered phosphate electrolytes was tested by electrochemical methods, *in-situ* ellipsometry, and atomic force microscopy [7]. These pH electrodes have been used for medical treatments and disease diagnosis [6,10,15,19,20] and re-evaluation of microelectrode methodology for in-vitro pH determination [11,21,22], among others.

The response, sensitivity, and reproducibility of the Sb-Sb-oxide electrode depend on the nature of oxide film developed on the Sb surface. Sb-Sb-oxide electrodes prepared from a single crystal in a nitrogen atmosphere showed better reproducibility and quick equilibrium attainment [8,16,17]. When the prepared Sb-electrode is immersed in an aqueous alkaline solution (e.g., 0.1 M Na_2CO_3) for about an hour, it quickly develops a thin Sb-oxide film on the surface [1,23,24]. Electrodes thus prepared by simple immersion method give a satisfactory pH response. Alternatively, the oxide can also be deposited electrochemically, namely anodic polarization, where a more precise and controlled oxide film is formed. It increases the electric field across the oxide film and leads to the growth of oxide by ionic conduction. The anodic polarization can be carried out at constant anodic potential (potentiostatic polarization) or constant anodic current (galvanostatic polarization) or by cyclic voltammetry (CV).

The preparation and characterization of polycrystalline Sb-Sb-oxide electrode is reported scarcely. This work focuses on the preparation of polycrystalline Sb-Sb-oxide electrodes at RT by electrochemical oxidation in different pH solutions. Electrochemical oxidation of the antimony electrode has been achieved in sulfuric acid as an acidic electrolyte, phosphate buffer as neutral, and borax buffer as a basic electrolyte. The composition of the differently prepared surface oxide has been studied using X-ray photoelectron spectroscopy (XPS) to explain its pH response effect.

2. EXPERIMENTAL

Antimony (Sb) powder (99.90%) was purchased from Fisher Scientific, India. The Sb powder was melted in a corning glass tube to prepare polycrystalline Sb ingot [12,23]. The ingot was then mounted on a Teflon rod with 4 mm of inner diameter to shape as an electrode (Fig. 1). Further, the exposed electrode surface was mechanically abraded with SiC paper until #2000 grit size to have a shiny surface. The electrode was then subjected to electrochemical oxidation in different pH solutions by potentiostatic, galvanostatic, and cyclic voltammetry (CV) to make an Sb-oxide layer on Sb. All the electrochemical polarizations were performed with an HA150 Hokuto Denko Potentiostat/Galvanostat, Japan, controlled by a self-made LabVIEW program. Different electrolytes with different pH were used to prepare the Sb-Sb-oxide electrodes. 5.0 M H_2SO_4, 0.5 M H_2SO_4, phosphate buffer solution of pH 7.0 (0.1 M NaH_2PO_4 + Na_2HPO_4,) and borax buffer of pH 10 were used for electrochemical oxidation. A series of buffer solutions from pH 2.0 to 10.0 were prepared and maintained with standard procedure[25].

The electrochemical measurements were carried out using a conventional three-electrode cell comprising the Sb-electrode as a working electrode, a saturated calomel electrode (SCE) as a reference and a platinum foil as a counter electrode. Potentiostatic polarization of the Sb-electrode was carried out at 2.0 V for 2 h. Similarly, a galvanostatic polarization was carried out at the current density of 4 mA/cm^2 until the potential reached 10 V. The process was repeated five times so that a sufficiently thick oxide layer could be formed. Regarding CV, in the case of H_2SO_4 solutions, the cathodic potential was fixed at -0.60 V while the anodic potential was varied as 0.80 V, 0.20 V, and 0.10 V to check the effect of anodic potential limit on the nature of the oxide. As for phosphate buffer (pH 7.0) and borax buffer solutions (pH 10.0), the potential range of CV was -0.60 V to 0.80 V as cathodic and anodic limits, respectively. CV was carried out at 0.01 V/s for each measurement. All the mentioned potential in this paper is referred to as SCE. All the chemicals were of reagent grade and purchased from Fisher Scientific, India. The solutions were prepared by dissolving an appropriate amount of chemical in double-distilled water.

The electrode response prepared by different methods was measured in buffer solutions of pH 2.0 to 10.0. The dynamic response of the electrodes was studied at pH 2.0, pH 7.0, and pH 10.0. The change in potential with time was recorded every 10 s for 30 min under stirring conditions.

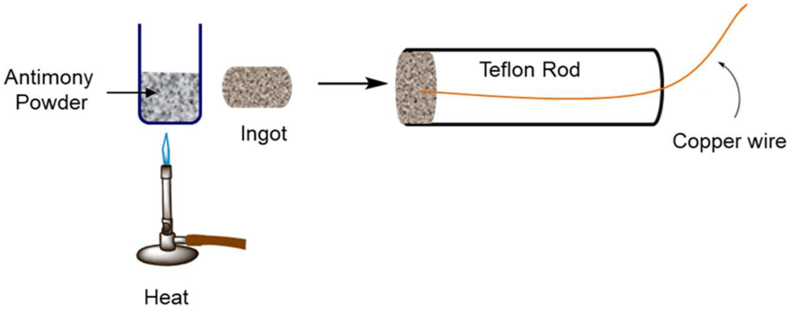

Fig. 1. Antimony ingot preparation scheme from powder sample

The Sb-oxide formed on the Sb-electrode by different methods was characterized by X-ray photoelectron spectroscopy (XPS). Before making measurements, the surface was sputtered by Ar^+ at 1.0 keV for 2 min to remove the surface impurities. The XPS measurement was then done on Sb-Sb-oxide samples prepared in 5.0 M H_2SO_4, phosphate buffer of pH 7.0, and borax buffer of pH 10.0 using a Thermo Scientific Sigma probe instrument in 2×10^{-9} mbar pressure. The X-ray source was Al Kα (1486.6 eV) with a beam size of 400 µm and a pass energy of 50 eV at 0.1 eV resolution. Fifty cycles of scanning were performed for collecting individual data. The spectra were fitted with Thermo Avantage software.

3. RESULTS AND DISCUSSION

3.1. Oxidation of Sb-electrode

Fig. 2a shows a CV of Sb electrode from +0.80 V to -0.60 V in 5.0 M and 0.5 M H_2SO_4 solutions. The current-potential response shows that the Sb dissolution starts at around -0.04 V and continues till +0.025 V. A shoulder appeared at +0.075 V till +0.137 V, which again increased till 0.190 V, and finally, a stable plateau continues from +0.325 V. These peaks correspond to the process of nucleation, formation, and expansion of a partly passivating oxide layer. A large limiting current afterward indicates the dissolution process through the passivation layer. The phenomena of Sb-dissolution in H_2SO_4 and phosphate solutions have already been reported [7,8].

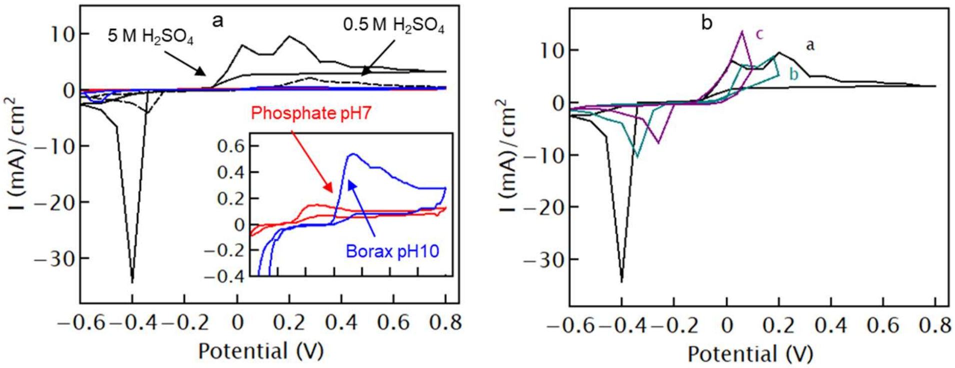

Fig. 2. Cyclic voltammetry of Sb electrode a) in 5 M and 0.5cM H_2SO_4 inset: zoom-in of phosphate buffer and borax buffer solution and b) Effect of anodic limits on the CV in 5.0 M H_2SO_4 (a= 0.8 V to -0.6V, b= 0.2 V to -0.6 V, c= 0.1 to -0.6 V)

The anodic current from -0.04 V to +0.45 V is attributed to the electro-formation of Sb_2O_3 via the formation of different soluble Sb species, while the steady-state current after +0.45 V is attributed to the anodic growth of the oxide [2,3]. The anodic growth of the Sb_2O_3 film occurred due to an ionic conduction mechanism caused by a ‘‘high field”, which drives the ionic migration in typical ‘‘valve” metals [26]. The formation of pentavalent Sb-oxide happens together with the oxygen evolution, confirmed by a ring-disc experiment [26]. In the case of 0.5 M H_2SO_4, anodic dissolution of Sb starts at +0.17 V till +0.29 V, the current gradually decreases, and finally, a sizeable steady-state current is observed after +0.325 V. This phenomenon shows only one type of Sb_2O_3 film formation by an ionic conduction mechanism [16,27].

During the cathodic scan, the current maintains an anodic value initially, showing the dissolution of antimony. As the potential moves to a more cathodic value, a pronounced cathodic peak due to the reduction of previously formed oxide in the anodic scan is observed at -0.40 V in 5.0 M and -0.30 V in 0.5 M H_2SO_4. There is not a distinct difference in the reduction peak in both solutions. However, the current in the 5.0 M H_2SO_4 solution is higher than in the 0.5 M H_2SO_4 solution. This indicates a high dissolution, and hence solubility of Sb is relatively large in high concentrated H_2SO_4 solution.

Similar CVs were performed in a phosphate buffer solution of pH 7.0 and a borax buffer of pH 10.0 to check the effect of the solution on the Sb-oxide formation (inset Fig. 2a). The dissolution and passivation current decreased by approximately 40 times in phosphate buffer and about 10 times in borax buffer compared to that in 5.0 M H_2SO_4 solution. This is due to the low dissolution of antimony in these solutions, and the formation of a stable phosphate and borax complex on the surface takes place. Interestingly, dissolution potential in the phosphate solution shifted to a negative potential by about 0.30 V, and the cathodic peak appeared very small compared to the other two solutions. It may indicate the formation of a stable phosphate complex on the surface and more stability of aqua Sb-ion in the phosphate solution. To understand the contribution of anodic peaks on the appearance of a cathodic peak, two different CVs were recorded at anodic potential limits of 0.20 V and 0.10 V at the same cathodic limit of -0.60 V, Fig. 2b. The appearance of a cathodic peak when the scan was reversed at the anodic limit of 0.10 V confirmed the dissolution of Sb and reduction of the anodically formed oxide film. Therefore, the dissolution of Sb takes place at about 0.0 V vs. SCE.

The approximate estimation of anodic and cathodic charges from CVs in various solutions shows that the anodic charge is only slightly larger than the cathodic charge in the case of H_2SO_4. Moreover, the charge difference was more significant in higher concentrations compared to the lower ones. This can be explained by considering the stability of oxide and reduction of Sb-ion during the cathodic scan. Since the dissolution rate in the 5.0 M H_2SO_4 solution is higher than in the 0.5 M H_2SO_4 solution, more Sb gets dissolved in the form of a trivalent or pentavalent ion and a thicker oxide layer may form [11,28,29]. All Sb-ions cannot be deposited back on the electrode surface during the cathodic scan due to the limitation imposed by diffusion co-efficients of aqua Sb-ions. Therefore, a smaller cathodic peak and hence lower cathodic charge density can be expected. When the potential is returned from either 0.20 V or 0.10 V, the anodic and cathodic charge densities are almost identical. This is because the reverse potential is very close to the start of the reduction potential of Sb-ion. So limited time is available for the dissolved Sb-ion to go into the solution before it is reduced back to Sb during the cathodic scan.

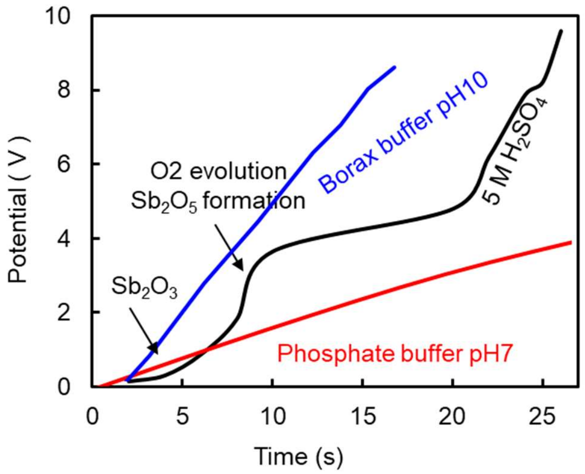

Fig. 3. Potential-time curve of Sb electrode during galvanostatic oxidation

In contrast, the ratio of anodic to cathodic charge is much higher in phosphate buffer. It indicates a meager amount of Sb dissolution; therefore, less Sb-ion is reduced back to the Sb surface during the cathodic scan. It shows a high stability of Sb in phosphate buffer compared to the acidic or alkaline media, and it might not be reducible or requires large overpotential. Thus, the oxidation of Sb in phosphate solution shows irreversible nature, and anodic polarization shows passivation of the electrode surface. The difference between peak potentials (anodic and cathodic) indicates the incomplete reversible oxide formation process in all the cases.

Galvanostatic polarization was carried out at 4 mA/cm^2 until the potential reached 10 V in 5.0 M H_2SO_4, phosphate buffer of pH 7.0, and borax buffer of pH 10.0. The process was repeated five times without taking out the electrode from the solution. Fig. 3 shows the results of the galvanostatic oxidation of Sb in the mentioned solutions. A systematic change of potential in the 5.0 M H_2SO_4 solution leading to the development of three distinct plateau regions can be seen. The first plateau from 0.0 to 0.30 V and the second plateau from 0.30 V to 1.7 V are assigned to continuous formation of Sb_2O_3 and thickening up to 1.7 V. The potential increment from 1.7 V until 4.5 V might be due to oxygen evolution and Sb_2O_5 formation. Thereafter, the exponential rise of current above 4.5 V is due to the thickening of the Sb-oxide layer. El Wakkad and Hickling [28] and Laihonen *et al.* [26] reported that the oxide layer formed on Sb under anodic polarization in an acidic medium consisted mainly of Sb_2O_3, under which a film of Sb_2O_5 in direct contact with Sb metal was produced later. The potential-time plots in phosphate and borax solutions do not show features like in the H_2SO_4 solution due to passive oxide formation, which leads to an exponential increase of potential.

For potentiostatic polarization, the Sb electrode was polarized anodically at 2.0 V for 2 h, and the change in current was recorded (plot not shown here). As the growth of oxide occurred, the current decreased and reached steady state (50 μA) after a short time interval, indicating for the dissolution of Sb under the passive film. The electro-formation of oxide was considered to take place in different steps until the trivalent oxide formation only.

3.2. Electrode surface characterization by XPS

XPS measurement was performed to characterize the surface state of Sb-Sb-oxide formed in three different media. The analysis was performed for O 1s and Sb 3d core levels spectra to detect the trivalent and pentavalent Sb-oxides [29]. Fig. 4 shows the XPS spectra of Sb 3d5/2 and Sb 3d3/2 core levels. Two different Sb-oxides, Sb_2O_3 and Sb_2O5 for 3d5/2, appear at 529.9 eV and 530.9 eV, respectively, and other spin pairs 3d3/2 appear at approximately 9.3 eV apart from their 3d5/2 peaks [30]. The approximate atomic percentage of Sb_2O_3 and Sb_2O_5 are 49% and 51%, 13% and 87%, and 70% and 30% in 5.0 M H_2SO_4, phosphate buffer (pH 7.0) and borax buffer (pH 10.0), respectively. The XPS analysis indicates that Sb-oxidation in an acidic medium leads to the formation of an equal amount of Sb_2O_3 and Sb_2O_5 on its surface. However, the oxide ratio is different in the electrode prepared in neutral phosphate buffer where Sb_2O_5 is 87 % in the total oxide layer. It means a stable Sb_2O_5 layer dominates the oxide composition.

In contrast, the Sb surface oxidized in alkaline media shows the presence of Sb_2O_3 dominated surface. Comparing three different media, the results indicate that the oxide formation is the highest in phosphate buffer compared to the borax buffer and sulfuric acid solution. This is due to the higher stability of the Sb-phosphate complex. The presence of phosphorous at 134.0 eV in the survey spectra (not shown here) suggests phosphate complex formation in the phosphate medium.

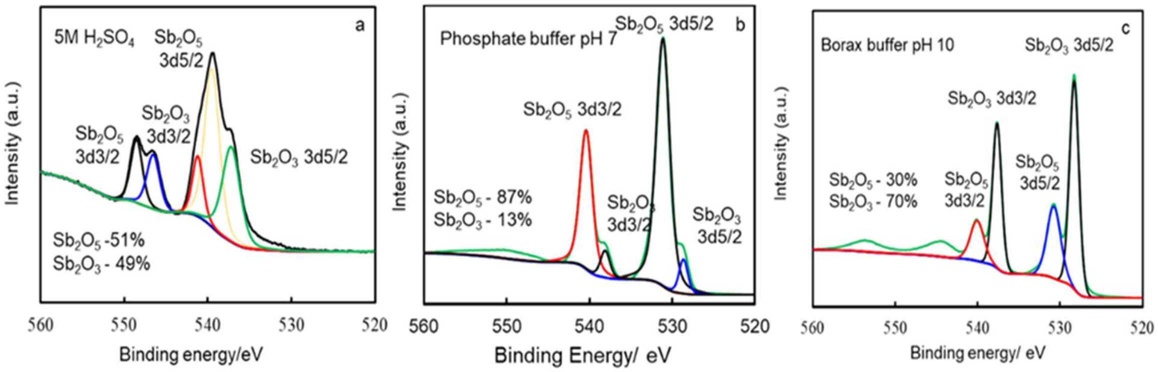

Fig. 4. XPS spectra of Sb-Sb-oxide electrode surfaces prepared in a) In acidic, b) neutral and c) basic solution

3.3. Response characterization of Sb-Sb-oxide sensor

3.3.1. Nernst response

Nernst response of differently prepared Sb-Sb-oxide electrodes was tested by pH measuring of a known buffer solution. The *e.m.f.* of the cell as a function of pH was recorded. Fig. 5 shows the cell *e.m.f* vs. pH plot of Sb-Sb-oxide electrodes prepared in different pH media by CV, potentiostatic polarization, and galvanostatic polarization. All electrodes show a linear potential response in the pH range of 2.0-10.0 irrespective of preparation methods. However, a slight difference in the value of the slope is observed in each electrode. The Nernst slope in 5.0 M H_2SO_4, phosphate buffer of pH 7.0, and borax buffer of pH 10.0 ranges from 0.050-0.052 V/pH, 0.048-0.050 V/pH, and 0.050-0.51 V/pH, respectively. The best Nernst slope is shown by the electrode prepared by the galvanostatic polarization method, and a relatively lower slope is exhibited by the electrodes prepared in phosphate buffer (see Table 1). This difference might be due to the Sb-Sb-oxide surface condition. The XPS analysis of the oxide formed in phosphate buffer showed 13 % and 87 % of Sb_2O_3 and Sb_2O_5, respectively. Therefore, it can be assumed that the response of the electrode is affected by the relative amounts of trivalent and pentavalent Sb-oxides. Further, in-depth surface characterization needs to be done to understand the role of the distribution of Sb-oxides on the Nernstian response. Another possibility for showing a lower slope might be the formation of a passive phosphate complex of antimony.

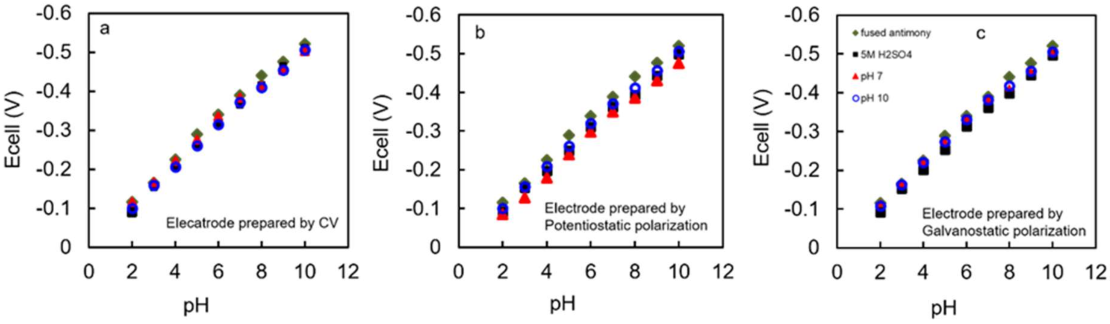

Fig. 5. Potential *vs.* pH response of the Sb-Sb-oxide electrodes prepared by a) CV, b) potentiodynamic polarization, and c) Galvanostatic polarization

Table 1. Nernst's Parameters of Sb-Sb-oxide electrodes oxidized by electrochemical process

Preparation method	Nature of Electrode	Slope (±1mV/pH)	Regression coefficient (R^2)	Standard potential (E^o) mV
-	Fused Sb electrode	-51	0.995	221
Cyclic voltammetry	5.0 M H_2SO_4 solution	-50	0.998	241
	Phosphate solution pH 7	-48	0.993	214
	Borax solution pH10	-50	0.994	226
Galvanostatic polarization	5.0 M H_2SO_4 solution	-52	0.998	245
	Phosphate solution pH 7	-49	0.993	255
	Borax solution pH 10	-50	0.998	235
Potentiostatic polarization	5.0 M H_2SO_4 solution	-50	0.997	241
	Phosphate solution pH 7	-50	0.995	236
	Borax solution pH 10	-51	0.997	236

The *e.m.f. vs.* pH plots are linear, with regression coefficients of more than 0.993 for all electrodes. The obtained slope is slightly lesser than expected from the Nernst equation. The electrode prepared by simple immersion in alkaline solution (pH 10.0) for 1 h has shown a slope of 0.51 V/pH; it attained equilibrium quickly, and the potential varied marginally over a more extended period [23,24]. The electrodes prepared by electrochemical oxidation also give reproducible results with quick attainment of equilibrium. However, electrochemically deposited Sb-oxides dissolve with frequent use and aging. Oxidation at higher potential or higher current density for a more extended period enhances the stability and durability of such

Sb-Sb-oxide electrodes. Unlike the simple fusion electrodes, the electrodes oxidized electrochemically do not require preconditioning in a solution of pH 10.0 before their use, which is an essential improvement regarding the use of such pH sensors for practical applications.

The standard potential of the Sb-Sb-oxide electrode varies with the electrode preparation method as well as with aging. This necessitates calibration of the electrode before use.

3.3.2. Dynamic-time response

Fig. 6. shows a dynamic time-response of the differently prepared electrodes. The equilibrium potential is attained within 2 min of immersion in the respective buffer solution. Interestingly, an equilibrium potential is attained only in about 10 min by the electrode prepared in the neutral media (phosphate buffer). Therefore, it clarifies that although the linear pH range and the slope are not significantly different, the response time is significantly longer in the electrode prepared in phosphate buffer. This time-delay to attain equilibrium potential might be due to the formation of a passive phosphate complex containing a more substantial amount of pentavalent Sb-oxide, as revealed by XPS analysis.

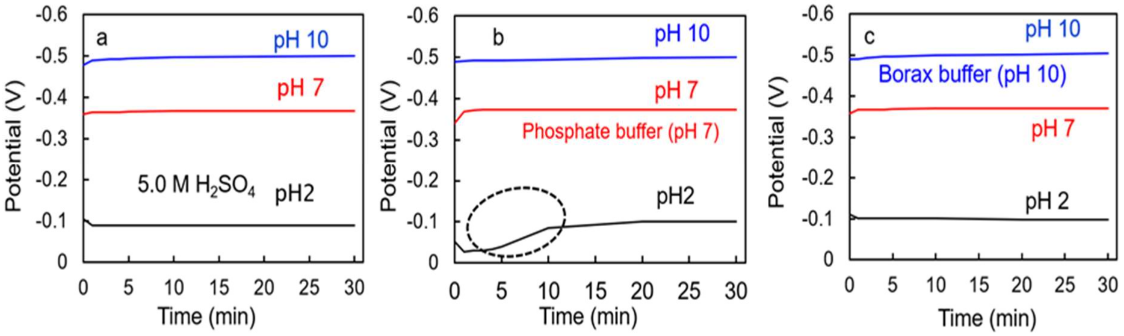

Fig. 6. Dynamic time-response of different Sb-Sb-oxide electrode prepared in a) in acidic, b) neutral and c) basic solution

4. CONCLUSION

The present work reveals the significance of electrochemical oxidation methods and electrolytic medium in preparing the Sb-Sb-Oxide pH electrode. The current-potential response showed a stepwise electro-formation of different Sb-oxides. XPS analysis reveals the presence of mixed oxides on the surface where Sb_2O_3 and Sb_2O_5 are almost similar in the electrode prepared in an acidic medium. The electrode prepared in a neutral phosphate buffer solution showed Sb_2O_5 dominated surface, while the one prepared in a basic borax buffer solution showed the presence of Sb_2O_3 dominated oxide.

The prepared Sb-Sb-oxide electrodes show reproducible pH values with a gradient of 0.049 – 0.052 V/ pH in pH range 2.0-10.0, and they are well suited to be used in pH measurements within the accuracy of ±0.02 pH. It also shows reproducible results with quick attainment of equilibrium in acidic and alkaline solutions. However, electrochemically deposited oxide dissolves with its frequent use and with aging. On a positive note, the electrodes prepared by electrochemical oxidation do not require preconditioning. The Sb-Sb-oxide electrode prepared in phosphate buffer (pH 7.0) gives a lower slope value, and it attained the equilibrium cell *e.m.f* slowly than the two others. This indicates the formation of a stable passive complex between antimony and phosphate. A detailed surface characterization of the Sb-oxide film may be required to further understand the role of different surface oxides in the response and life of the electrode.

Decelerations

Competing Interests: The authors declare no competing interests.

Funding: The project was funded by the Central Department of Chemistry, Tribhuvan University, Kirtipur, Kathmandu, Nepal

Data Availability: The supplementary data and information of this study are available from the corresponding author upon reasonable request.

Acknowledgments

The authors would like to thank the Central Department of Chemistry, Tribhuvan University, Nepal, for making available laboratory facilities and the National Institute of Materials Science, Tsukuba, Japan, for providing the XPS facilities.

REFERENCES

[1] S. Głab, A. Hulanicki, G. Edwall and F. Ingman, Critical Rev. in Anal. Chem. 21 (1989) 29.
[2] A. Uhl and W. Kestranek, Monatshefte fur Chemie 44 (1923) 29 .
[3] S. P. L. Sörensen, Biochem. Z. 21 (1909) 131.
[4] G. McLauchlan, J. M. Rawlings, M. L. Lucas, R. F. McCloy, G. P. Crean and K. E. McColl, Gut. 28 (1987) 935.
[5] J. Kong, S. Shi, X. Zhu and J. Ni, J. Environ. Sci. 19 (2007) 1380 .
[6] I. Kleinberg, G. N. Jenkins, R. Chatterjee and L. Wijeyeweera, J. Dent. Res. 61 (1982) 1139.
[7] O. E. Linarez Pérez, O. E. L. Pérez, M. A. Pérez and M. L. Teijelo, J. Electroanal. Chem. 632 (n.d.) 64.
[8] M. Metikoš-Huković, R. Babić and S. Brinić, J. Power Sources 157 (2006) 563 .
[9] J. Soltis and K. A. Lichti, Corr. Sci. 68 (2013) 162 .
[10] J. T. Stock, W. C. Purdy and L. M. Garcia, Chem. Rev. 58 (1958) 611 .
[11] G. Edwall, Med. Biol. Eng. Comput. 16 (1978) 661.

[12] Y. Ha and M. Wang, Electroanalysis 18 (2006) 1121 .

[13] C. L. P. S. Zanta, P. A. Michaud, C. Comninellis, A. R. De Andrade and J. F. C. Boodts, J. Appl. Electrochem. 33 (2003) 1211 .

[14] D. Li, J. Tang, X. Zhou, J. Li, X. Sun, J. Shen, L. Wang and W. Han, Chemosphere 149 (2016) 49.

[15] G. Malnic and F. L. Vieira, Yale J. Biol. Med. 45 (1972) 356.

[16] S. Kallip, P. Laukkanen, A. Jänes, V. Sammelselg, J. Väyrynen, P. Miidla and E. Lust, Surface Science 532–535 (2003) 1121.

[17] E. Kinoshita, F. Ingman, G. Edwall, S. Thulin and S. Głąb, Talanta 33 (1986) 125 .

[18] T. R. Ball, Trans. Electrochem. Soc. 72 (1937) 139 .

[19] F. Sjöberg, G. Edwall and N. Lund, Scandinavian J. Clinical and Laboratory Investigation 47 (1987) 11.

[20] M. R. H. F. L. Rosenfeldt, J. A. Smith, D. E. Mulcahy and J. T. Bannigan, J. Med. Eng. Technol. 23 (1999) 119.

[21] J. B. Puschett and P. E. Zurbach, Kidney Int. 6 (1974) 81 .

[22] A. V. Beran, R. F. Huxtable and D. R. Sperling, J. Appl. Phys. 41 (1976) 442.

[23] R. R. Pradhananga and M. Pradhananga, J. Nep. Chem. Soc. 16 (1997) 30.

[24] R. R Pradhananga and K. Parajuli, J. Nep. Chem Soc. 17 (1998) 22.

[25] R. A. Alberty and R. J. Silbey, Physical chemistry, 2nd ed., Wiley, New York (1997).

[26] S. Laihonen, T. Laitinen, G. Sundholm and A. Yli-Pentti, Electrochim. Acta 35 (1990) 229.

[27] M. T. Flanagan and N. J. Carroll, Biotechnol. Bioengin. 28 (1986) 1093.

[28] S. E. S. E. Wakkad and A. Hickling, J. Phys. Chem. 57 (1953) 203.

[29] D. Briggs, Handbook of X-ray Photoelectron Spectroscopy C. D. Wanger, W. M. Riggs, L. E. Davis, J. F. Moulder and G. E. Muilenberg Perkin-Elmer Corp., Physical Electronics Division, Eden Prairie, Minnesota, USA (1979). Pp. 190 pp.

[30] J. F. Moulder, W. F. Stickle, P. E. Sobol and K. D. Bomben, Handbook of XPS (1995) pp. 255.